ESMO GOOD SCIENCE BETTER MEDICINE BEST PRACTICE

ESMO IMMUNO-ONCOLOGY AND TECHNOLOGY

ORIGINAL ARTICLE

Durable complete response after combined treatment with tumor-infiltrating lymphocytes and oncolytic adenovirus (TILT-123) in a patient with metastatic mucosal melanoma

T. J. Monberg[1], T. Kudling[2†], B. Albieri[1†], S. Pakola[2], E. Ellebaek[1], M. Donia[1], R. L. Eefsen[1], C. von Buchwald[3], C. Kistler[4], J. M. Santos[2,4], J. Clubb[2,4], L. Haybout[2,4], M. C. W. Westergaard[1], D. C. A. Quixabeira[2,4], E. Jirovec[2], R. Havunen[2,4], S. Sorsa[2,4], V. Cervera-Carrascon[2,4], A. Hemminki[2,4,5] & I. M. Svane[1*]

[1]National Center for Cancer Immune Therapy (CCIT-DK), Department of Oncology, Copenhagen University Hospital, Herlev, Denmark; [2]Cancer Gene Therapy Group, Translational Immunology Research Program, University of Helsinki, Helsinki, Finland; [3]Department of ORL, Head and Neck Surgery and Audiology, Copenhagen University Hospital, Rigshospitalet, Denmark; [4]TILT Biotherapeutics Ltd, Helsinki; [5]Helsinki University Hospital Comprehensive Cancer Center, Helsinki, Finland

Available online 12 August 2024

Background: Despite significant advancements in the treatment of malignant melanoma, metastatic mucosal melanoma remains a therapeutic challenge due to its complex pathogenesis, distinct pathological characteristics, and limited response to immunotherapy. Combining different immunotherapeutic approaches offers a potential strategy to address these challenges. Tumor-infiltrating lymphocyte (TIL) therapy and oncolytic virus therapy represent promising treatment modalities that may synergize with each other.

Patient and methods: We present a case of a 48-year-old woman with metastatic sinonasal mucosal melanoma who achieved a durable complete pathological response following treatment with multiple injections of the oncolytic virus TILT-123 (igrelimogene litadenorepvec) and a single infusion of TILs, without preconditioning chemotherapy or postconditioning interleukin-2.

Results: Immunohistochemical analysis and single-cell sequencing revealed interesting alterations in injected and noninjected tumors as well as in peripheral blood, during the treatment course, suggesting that TILT-123 facilitated TIL engraftment into the tumor, ultimately leading to a complete response.

Conclusions: This case underscores the potential of combined immunotherapeutic approaches as a promising strategy for patients with metastatic mucosal melanoma.

Key words: case report, mucosal melanoma, tumor-infiltrating lymphocytes, oncolytic virus therapy

INTRODUCTION

Mucosal melanoma is an aggressive histological subtype associated with low overall survival and a poor treatment response. Its incidence varies widely, comprising 1% of melanomas in Europe and up to 20% in Asia.[1,2] It originates from melanocytes covering mucosal membranes, with the head and neck region being the most common site.[3] The pathogenesis of mucosal melanoma is poorly understood, and its genetic profile differs from cutaneous melanoma, with a lower mutational burden and a lower frequency of BRAF V600 mutations.[4,5] While the treatment of cutaneous melanomas was revolutionized with the introduction of immune checkpoint inhibitors (ICIs), robust evidence of the efficacy of ICI in mucosal melanoma is still awaited. Surgery, with or without radiation, remains the primary choice for local disease, while metastatic treatment primarily relies on the evidence obtained in the treatment of metastatic cutaneous melanoma. Treatment with tumor-infiltrating lymphocytes (TILs) was recently proven to be effective in patients with cutaneous melanoma resistant to anti-programmed cell death protein 1 (anti-PD-1) therapy[6] and promising results of TIL therapy in noncutaneous melanoma have been reported.[7,8] However, still these tumors represent a considerable therapeutic challenge.

The 5-year overall survival for mucosal melanoma is reported to be <25%, with minimal improvement over the past decades and a high rate of recurrence (50%-70%).[9] Further, patients with mucosal melanoma are often excluded from clinical trials, and the amount of data on new and effective treatment modalities is limited.

*Correspondence to: Prof. Inge Marie Svane, National Center for Cancer Immune Therapy (CCIT-DK), Herlev Hospital, Borgmester Ib Juuls Vej 13, 2730 Herlev, Denmark. Tel: +45-38-68-21-31

E-mail: inge.marie.svane@regionh.dk (I. M. Svane).

†These authors contributed equally to this work.

2590-0188/© 2024 The Author(s). Published by Elsevier Ltd on behalf of European Society for Medical Oncology. This is an open access article under the CC BY-NC-ND license (http://creativecommons.org/licenses/by-nc-nd/4.0/).

Oncolytic viruses (OVs) infect and lyse cancer cells, resulting in exposure of tumor antigens to immune cells in the tumor microenvironment (TME). Talimogene laherparepvec (T-VEC) has been approved by the Food and Drug Administration (FDA) and European Medicines Agency (EMA) for the treatment of advanced melanoma but the systemic efficacy of OV monotherapy has generally been modest. Because of immunological synergies, the full anticancer effects of OVs can possibly be unleashed when combined with other types of immunotherapy.[10] The combination of pembrolizumab and OV showed promising results in a phase IIb trial, but no benefit on progression-free survival or overall survival could be demonstrated in the phase III part of the trial.[11] Thus there is a lack of robust evidence demonstrating the efficacy of OV in the context of combination immunotherapy.

To date, combined treatment with OV therapy and TIL therapy remains unexplored.

TILT-123 (igrelimogene litadenorepvec, Ad5/3-E2F-d24-hTNFa-IRES-hIL2) is an oncolytic adenovirus with the ability to replicate selectively in cancer cells and engineered to express two transgenes coding for human interleukin-2 (IL-2) and tumor necrosis factor-alpha (TNF-α) upon replication. TILT-123 is designed to stimulate the immune infiltration into the tumor and enhance cytotoxic T-cell activity.

We report the case of a 48-year-old woman with a durable clinical complete response after combined treatment with TIL therapy and oncolytic adenovirus TILT-123 for ICI-resistant metastatic sinonasal mucosal melanoma in the clinical trial NCT04217473 (TILT-T215).

CASE PRESENTATION

A 48-year-old woman, with known von Willebrand disease and a history of months of self-limiting epistaxis, presented with advanced primary sinonasal mucosal melanoma with a primary tumor almost completely blocking the left nasal cavity. The tumor was positive for MelanA and S100, BRAF wild type, and programmed death-ligand 1 (PD-L1) expression was $<1\%$. Positron emission tomography/computed tomography (PET/CT) revealed three PET-positive suspicious lymph nodes on the left side of the neck. One of these lymph nodes was extirpated for pathological examination which confirmed metastasis from malignant mucosal melanoma. The patient was considered for surgery but was nonoperable and treatment with ipilimumab/nivolumab was initiated. Unfortunately, the patient progressed after seven cycles (four cycles of combination therapy and three cycles of nivolumab monotherapy). The best overall response was stable disease.

Nine weeks after the last dose of nivolumab the patient was enrolled in the trial. The treatment schedule is outlined in Figure 1. At baseline, the patient had three tumor lesions: one primary tumor in the left nasal cavity and two metastases to cervical lymph nodes on the left side (Figure 2). One of the lymph node metastases was resected for TIL production on day -5 and histological analysis confirmed metastasis from malignant melanoma. The first treatment with TILT-123 was administered intravenously (i.v.; day 1) at a dose of 3×10^{11} viral particles. Intratumoral (i.t.) injections at a dose of 1×10^{11} viral particles were administered in the remaining lymph node metastasis on days 8, 22, 36, 50, and 64. The primary tumor in the nasal cavity remained uninjected with virus, but was available for biopsies throughout the trial. On day 43, autologous TILs were reinfused i.v. without prior lymphodepleting chemotherapy or postinfusion IL-2. On day 36, before the administration of TILs, the patient had stable disease according to RECIST version 1.1 with a 14% decrease in the tumor burden. Importantly, both the injected and noninjected tumors showed regression (20% and 10%, respectively). On day 78, after TIL infusion, the patient developed a partial response with a 37% decrease in tumor burden (50% and 29% in the injected and noninjected tumor, respectively) She was then enrolled in an extension phase of the trial allowing for further i.t. injections with TILT-123 every third week up to 2 years. She received eight more injections with TILT-123. 270 days after enrollment, PET/CT suggested progressive disease with increased fludeoxyglucose uptake and a 35% size increase, compared with nadir, of the tumor lesion in the nasal cavity. PET/CT responses during the treatment course are shown in Figure 3. Based on the PET/CT findings, the tumor in the nasal cavity was surgically resected. In the histopathological examination, widespread inflammation with no malignant cells was observed (Figure 3). A biopsy, subsequently taken from the lymph node remnant on the left side of the neck, revealed no malignant cells. Thus the patient had a pathologically confirmed complete response. The patient is presently alive with no evidence of disease, >2.5 years from enrollment in the clinical trial.

No serious adverse events were registered during the treatment course. Adverse events were mild [Common Terminology Criteria for Adverse Events (CTCAE) grade 1], primarily fever and injection site pain.

The patient was treated in the phase I, dose-escalation trial NCT04217473 in which 17 patients with ICI-resistant metastatic malignant melanoma were treated with TILT-123 and TIL therapy. The dose-escalating regimen has previously been described.[12] The trial results are still unpublished.

PATIENT AND METHODS

Expansion of tumor-infiltrating lymphocytes

TILs were expanded *ex vivo* from the resected lymph node metastasis according to good manufacturing practice as described in Supplementary Text S1, available at https://doi.org/10.1016/j.iotech.2024.100726.

The final TIL infusion product contained 69.2×10^9 cells and was administered to the patient 48 days after tumor resection, 43 days after the first administration of TILT-123.

Virus distribution in blood, saliva, and urine

To assess the amount of virus in the peripheral blood, blood samples were taken before every treatment with TILT-123 and 1 and 16 h after treatment. Virus persistence was

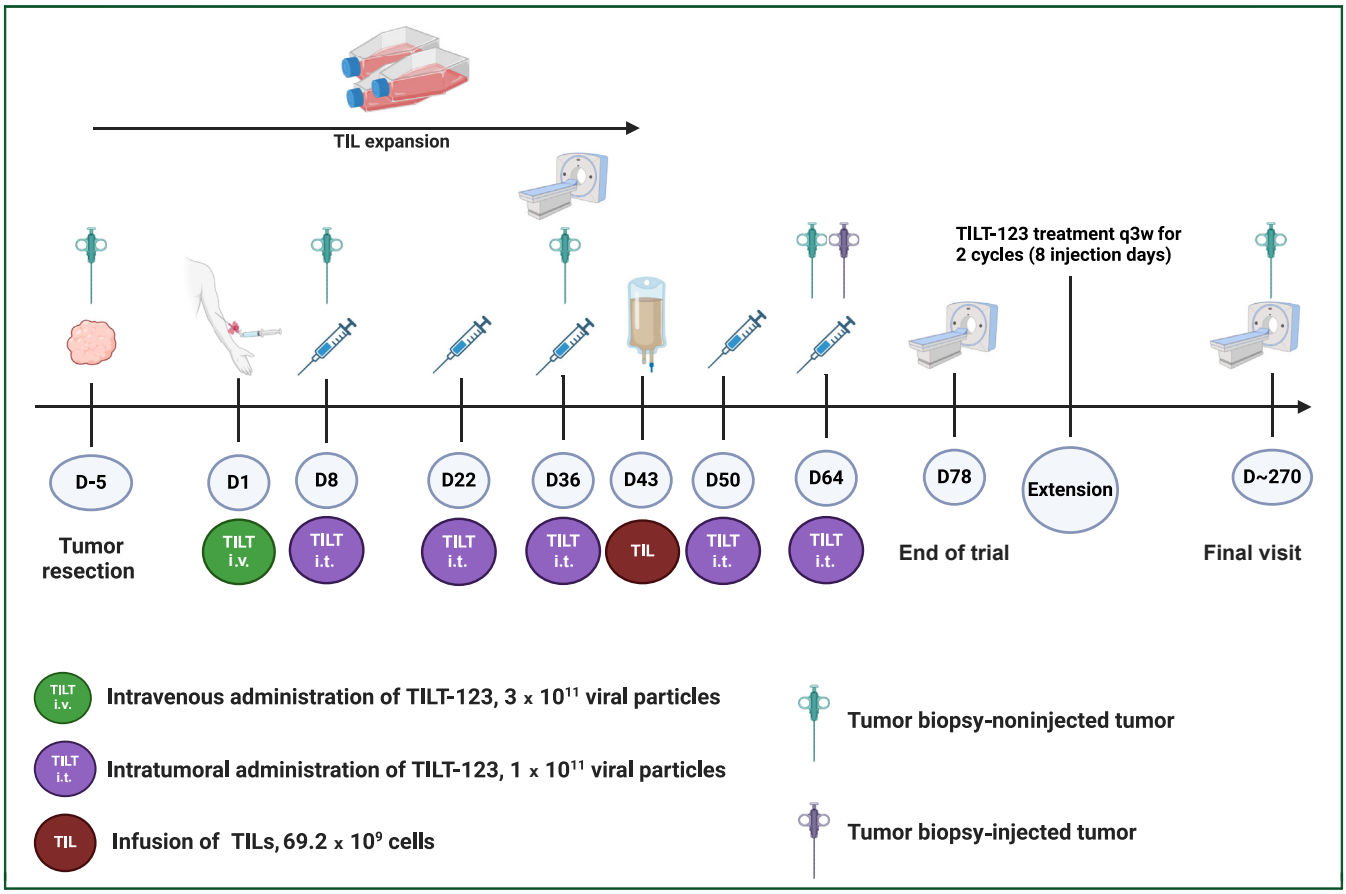

Figure 1. Treatment schedule in the trial NCT04217473. Numbers indicate 'days'. Tumor tissue for tumor-infiltrating lymphocyte (TIL) therapy was resected before inclusion in the trial (day −5). Expanded TILs were administered on day 43 after the first four injections [intravenous (i.v.) and intratumoral (i.t.)] of TILT-123. After TIL therapy the patient received two additional injections with TILT-123 before the end of the study evaluation. After the end of the study evaluation (day 78), the patient continued TILT-123 therapy with i.t. injections every third week for two treatment cycles. The final evaluation was carried out 270 days after treatment started. Biopsies from a noninjected tumor were carried out at baseline, day 8, day 36, day 64, and when the tumor was finally resected on day 270. A biopsy from the injected tumor was available from day 64. Created with BioRender.com.
q3w, every 3 weeks.

evaluated using quantitative polymerase chain reaction (qPCR) to determine the copy numbers of the virus genome. Further, serum samples were collected before treatment and 16 h after treatment to detect neutralizing antibodies generated against TILT-123.

To assess viral shedding, urine and saliva samples were collected before every treatment with TILT-123 and 16 h after treatment, and qPCR was used to determine the copy numbers of virus genomes.

Tumor biopsies

Tumor biopsies from the noninjected sinonasal tumor were carried out at baseline and on days 8, 36, and 64 of the treatment protocol. Tissue from the injected tumor (neck) subjected to biopsy was available only from day 64 (Figure 1). Further, for pathological examination, tissue from the noninjected tumor in the nasal cavity was available after the tumor resection carried out on day 270.

Phenotypic characterization of peripheral blood mononuclear cells and infusion product

Phenotypical changes were investigated in peripheral blood mononuclear cells (PBMCs) collected before study enrollment and at days 8, 36, and 64 during the treatment schedule. The method is described in Supplementary Text S2, available at https://doi.org/10.1016/j.iotech.2024.100726 and the panel of antibodies is illustrated in Supplementary Table S1, available at https://doi.org/10.1016/j.iotech.2024.100726.

Single-cell sequencing

A single-cell suspension of PBMCs and TIL infusion product was generated as described in Supplementary Text S3, available at https://doi.org/10.1016/j.iotech.2024.100726. This was followed by the construction of whole transcriptome and T-cell receptor libraries, single-cell processing, and finally, cell type annotation as described in the Supplementary Material (Supplementary Text S3, Figure S1, and Table S2), available at https://doi.org/10.1016/j.iotech.2024.100726.

Histology, immunohistochemistry, and image analysis

Tumor biopsies were formalin-fixed, paraffin-embedded, and sections were prepared for hematoxylin—eosin staining (HistologiX).

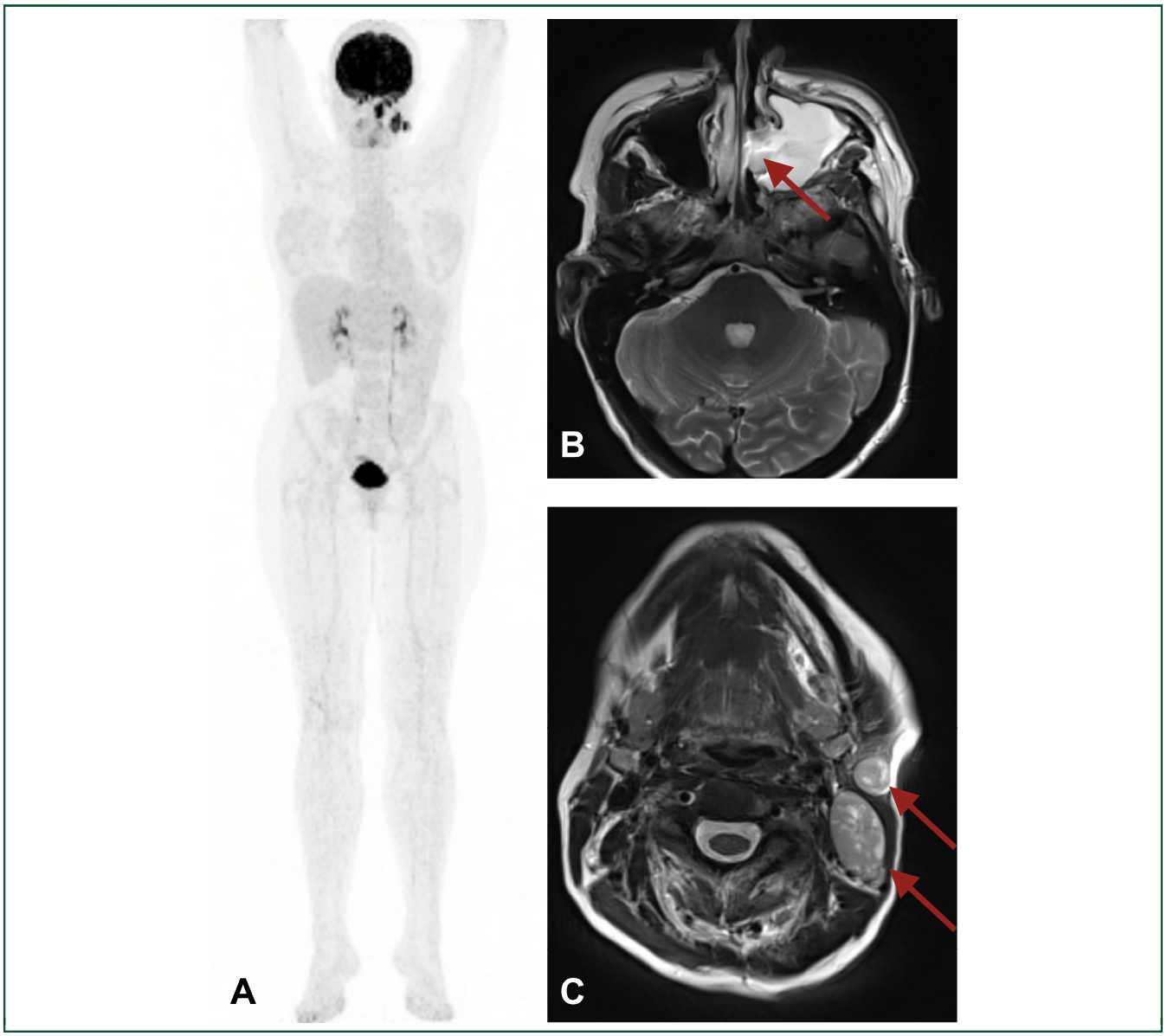

Figure 2. Tumor imaging at baseline. (A) Positron emission tomography (PET) scan showing the three PET-positive lesions localized to the left nasal cavity and lymph nodes on the left side of the neck. (B) Magnetic resonance (MR) scan, T2-weighted, showing the primary tumor blocking the left nasal cavity. (C) MR scan, T2-weighted, showing metastases in two lymph nodes on the left side of the neck.

PD-L1 single immunohistochemical (IHC), CD4/FOXP3 dual, and CD8/PD-1/Ki67 triple immunofluorescence (IF) staining was outsourced to Concept Life Sciences for analysis of changes in immune cell markers and detection of TILT-123. Before IHC and multiplex IF staining, hematoxylin—eosin images were annotated for TME regions by a pathologist at the Helsinki University Hospital (HUS). The staining method is described in Supplementary Text S4, available at https://doi.org/10.1016/j.iotech.2024.100726.

RESULTS

Phenotypic characterization of the TIL infusion product

The final TIL infusion product comprised 69.2 $\times$ 10^9 cells, with 93% being CD3+ cells, predominantly CD4+ cells (96.4%) and a smaller fraction of CD8+ cells (3.6%). The majority of both CD4+ and CD8+ cells were effector memory cells and most of them were positive for CD27, CD28, and CD39, consistent with a typical TIL product.[13] Reactivity assays using multicytokine intracellular staining with and without stimulation with interferon-gamma were unable to detect *in vitro* reactivity of the infused TILs against autologous tumor digest or tumor cell line.

Immunohistochemical analysis of tumor biopsies

Results from the IHC analyses of the tumor tissue are presented in Figure 4 and Supplementary Table S3, available at https://doi.org/10.1016/j.iotech.2024.100726. Biopsies from the noninjected tumor in the nasal cavity revealed an increased infiltration of CD8+ and CD4+ cells over the treatment course. The fraction of CD8+ cells increased from 0.03% at baseline to 1.52% on day 64, with a notable increase following TIL infusion. An increase in the fraction of

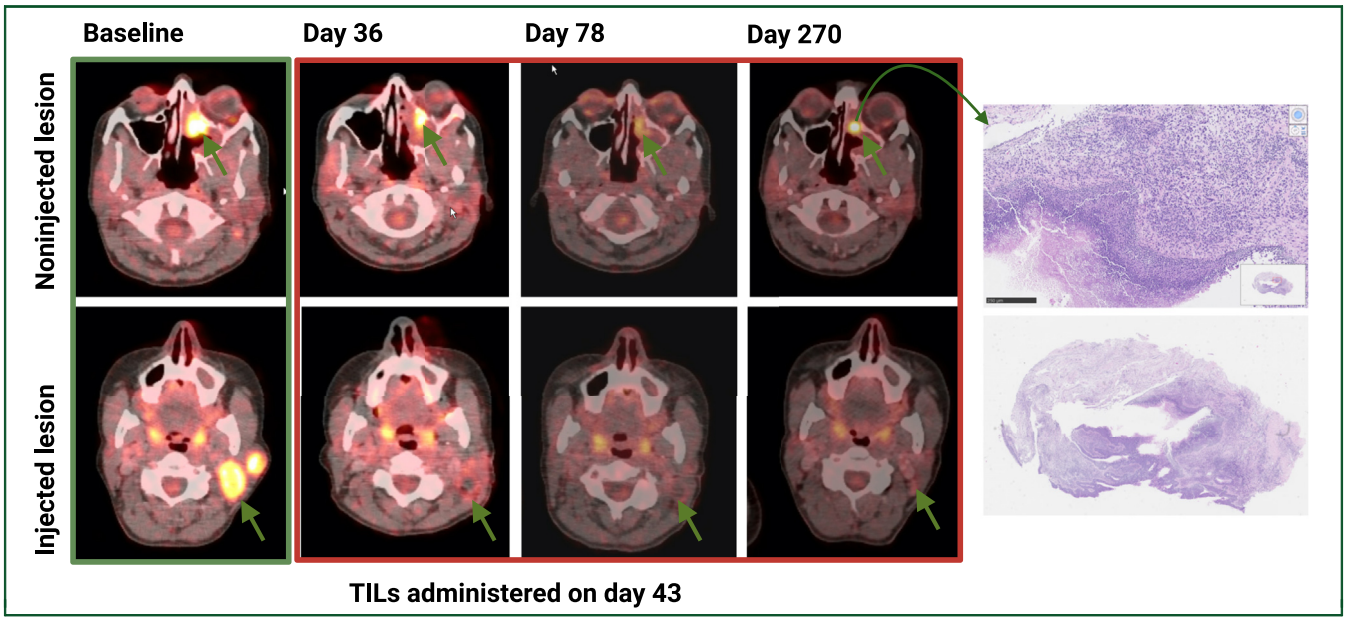

Figure 3. Positron emission tomography/computed tomography (PET/CT) imaging before and after treatment with TILT-123 and tumor-infiltrating lymphocyte therapy. The patient developed a partial response according to RECIST version 1.1 at the CT scan on day 78. After extension therapy with TILT-123, the PET scan showed increased glucose uptake at the tumor site in the nasal cavity. However, the pathology report showed a pathological complete response. Immunohistochemical analyses of resected tissue from the nasal cavity were carried out 270 days after treatment initiation. The tissue was characterized by edema and chronic inflammation without any cytological atypia or proliferation. There were no morphological or immunohistochemical signs of malignancy. These findings are compatible with a protracted inflammatory response in the tumor scar, perhaps contributing to a long disease-free survival.

CD8+ Ki67+ and CD8+PD-1+ cells was also seen during the treatment course, but in general, these cells were low in number.

The fraction of CD4+ cells in the noninjected tumor increased from 0.25% at baseline to 16.4% on day 64. Approximately half of these cells were FOXP3 negative. However, an increase in the fraction of CD4+FOXP3+ cells was also observed from 0.05% at baseline to 4.18% on day 64.

Tumor cells had an increased expression of PD-L1 on day 8 after the first i.v. injection with TILT-123, with most PD-L1+ cells being strongly positive. From days 8 to 64, the fractions of tumor cells expressing PD-L1 decreased from 35% to 21% and a shift from strong to weak expression of PD-L1 was observed.

Whole-transcriptome single-cell analysis

Cell composition of PBMC samples obtained on days −14 (D−14, baseline), 36 (D36), and 64 (D64) was highly similar and no treatment-specific cell clusters were observed (Figure 5). The TIL infusion product had a different phenotypic profile and almost exclusively comprised effector memory CD4+ T cells, confirming our previous results. The number of circulating natural killer (NK) cells, B cells, and central memory CD4+ T cells on D64 was increased by 53.7%, 46.6% and 48.8%, respectively, compared with baseline (Supplementary Table S2, available at https://doi.org/10.1016/j.iotech.2024.100726), while the number of naive T cells and T regulatory cells (Tregs) decreased by 67.3% and 63.4%, respectively. On day 36, these populations remained relatively stable.

Analysis of several cytotoxic markers showed higher expression of granzyme A (*GZMA*) and granzyme B (*GZMB*) in NK cells as well as lowered expression of Tim3 (*HAVCR2*) on D64 compared with baseline and D36. CD8+ T cells showed higher expression of granzyme H (*GZMH*) by D64, and the expression of *GZMA* was first lowered at D36 compared with D−14 and then increased again at D64. Further, we observed a steady decrease in the expression level of TIGIT and cytotoxic T-lymphocyte-associated protein 4 (CTLA-4) in Tregs.

Differentially expressed gene analysis and gene ontology analysis were carried out for NK, B, and CD8+ T cells on days 36 and 64 (Figure 5 and Supplementary Figure S2, available at https://doi.org/10.1016/j.iotech.2024.100726). All cell types showed high expression of *FKBP5* on day 36 which is linked to a proinflammatory profile and altered nuclear factor-kappa B (NF-κB)-related gene networks.[14] Indeed, we observed the upregulated expression of *NFKB1* and *NFKBIA* in NK and CD8+ T cells as well as *JADE3, SNX8,* and *SNX9* in B cells on day 36 compared with baseline. Overall, on day 36, we observed improved cell activation and differentiation, but reduced effector function and lowered survival.

On day 64, after TIL infusion, the phenotype of the cells showed a different pattern. We observed a shift in NK cells toward a more cytotoxic cell type and a shift in B cells toward a more mature cell type. Further, CD8+ T cells showed a shift toward a more effector phenotype (Supplementary Text S5, available at https://doi.org/10.1016/j.iotech.2024.100726 for more details).

TCR clonotype analysis

Analysis of T-cell receptor diversity is presented in Figure 6 and Supplementary Figure S3, available at https://doi.org/1

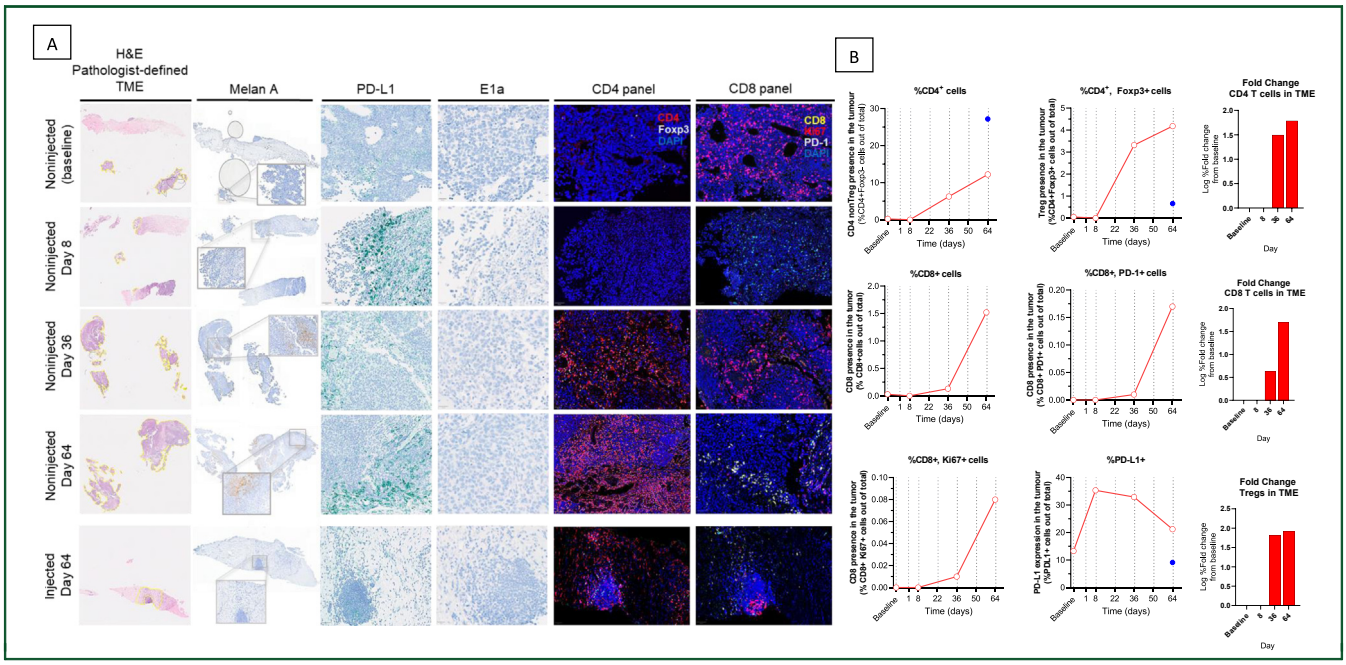

Figure 4. (A) Representative immunohistochemistry of tumor biopsies. Noninjected tumor biopsies taken at baseline (row 1), day 8 (row 2), day 36 (row 3), and day 64 (row 4), and one injected tumor biopsied at day 64 (row 5). Immunochemical staining includes hematoxylin—eosin (H&E) shown with pathologist-defined tumor microenvironment (TME; defined within the yellow boundaries; column 1); Melan A (column 2); programmed death-ligand 1 (PD-L1; column 3); adenovirus E1a (column 4); multiplex immunofluorescence (IF) panel 1 for CD4, Foxp3, and 4′,6-diamidino-2-phenylindole (DAPI; column 5); and multiplex IF panel 2 for CD8, Ki67, programmed cell death protein 1 (PD-1), and DAPI (column 6). (B) Graphical representations of Indica labs HALO-quantified IF staining showing percentage change in intratumoral populations of CD4+, CD4+ Foxp3+, CD8+, CD8+ PD-1+, CD8+ Ki67+, and PD-L1+. The most notable increase from baseline populations (CD4+, CD4+ Foxp3+, and CD8+) is also represented as bar charts in the far-right column.
Treg, T regulatory cell.

0.1016/j.iotech.2024.100726. PBMC samples showed a high diversity of the TCR repertoires, reaching 95%, 97%, and 95% of unique clonotypes, respectively, at baseline (D−14), day 36 (D36), and day 64 (D64). The TIL infusion product had higher clonality and the percentage of unique clonotypes was lower than in PBMCs (17%). The usage of β chain V and J genes in TCRs in the TIL sample was more uniform with the clear predominance of TRBV2-3*01/TRBJ1-2*01 combination. TCRs in PBMC samples were more heterogeneous; however, we identified two distinctive variants, having the same TRBJ2-01*1 chain and two V chains: TRBV9*01 and TRBV20-1*01.

We compared the most expanded TCRs and found that only one clonotype was similar between D64 and TIL samples. This clonotype appears in peripheral blood after TIL infusion, suggesting that it originates from the TIL product. However, it has not previously been described in VDJdb.[15]

D36 and D64 samples also showed specific TCR clonotypes appearing after the treatment; however, none of them were previously reported.

Detection of virus in blood, urine, and saliva

In peripheral blood, the virus was detected at a concentration between 10^2 VP/ml blood and 10^4 VP/ml blood after TILT-123 administration on days 1, 8, 22, and 36 of the protocol, with the highest concentration detected after i.v. administration of TILT-123. A similar increase was observed in the extension phase of the protocol. qPCR was negative right before the next virus injection (Supplementary Figure S4, available at https://doi.org/10.1016/j.iotech.2024.100726).

Viral genomes were detected in urine after the first i.v. treatment with TILT-123, but not at later timepoints (Supplementary Figure S5, available at https://doi.org/10.1016/j.iotech.2024.100726). It is not known if functional virus particles were present in urine. No viral genomes were detected in saliva (Supplementary Figure S6, available at https://doi.org/10.1016/j.iotech.2024.100726)

A low titer of neutralizing antibodies against the virus was detected at baseline. Seven days after i.v. treatment with TILT-123, the titer had increased and it remained high for the rest of the treatment course (Supplementary Figure S7, available at https://doi.org/10.1016/j.iotech.2024.100726).

DISCUSSION

Metastatic mucosal melanoma represents a significant therapeutic challenge. The efficacy of TIL therapy in this hard-to-treat patient population has been reported[8] but the considerable toxicity associated with high-dose chemotherapy and IL-2 limits the applicability of this treatment. The current case is the first to show that the combination of OV therapy and TILs without complimentary high-dose chemotherapy and IL-2 can result in a durable complete response in stage III malignant mucosal melanoma with minimal toxicity compared with classical TIL therapy.

A comprehensive panel of immune assessments sheds light on the mechanisms underlying this response. The

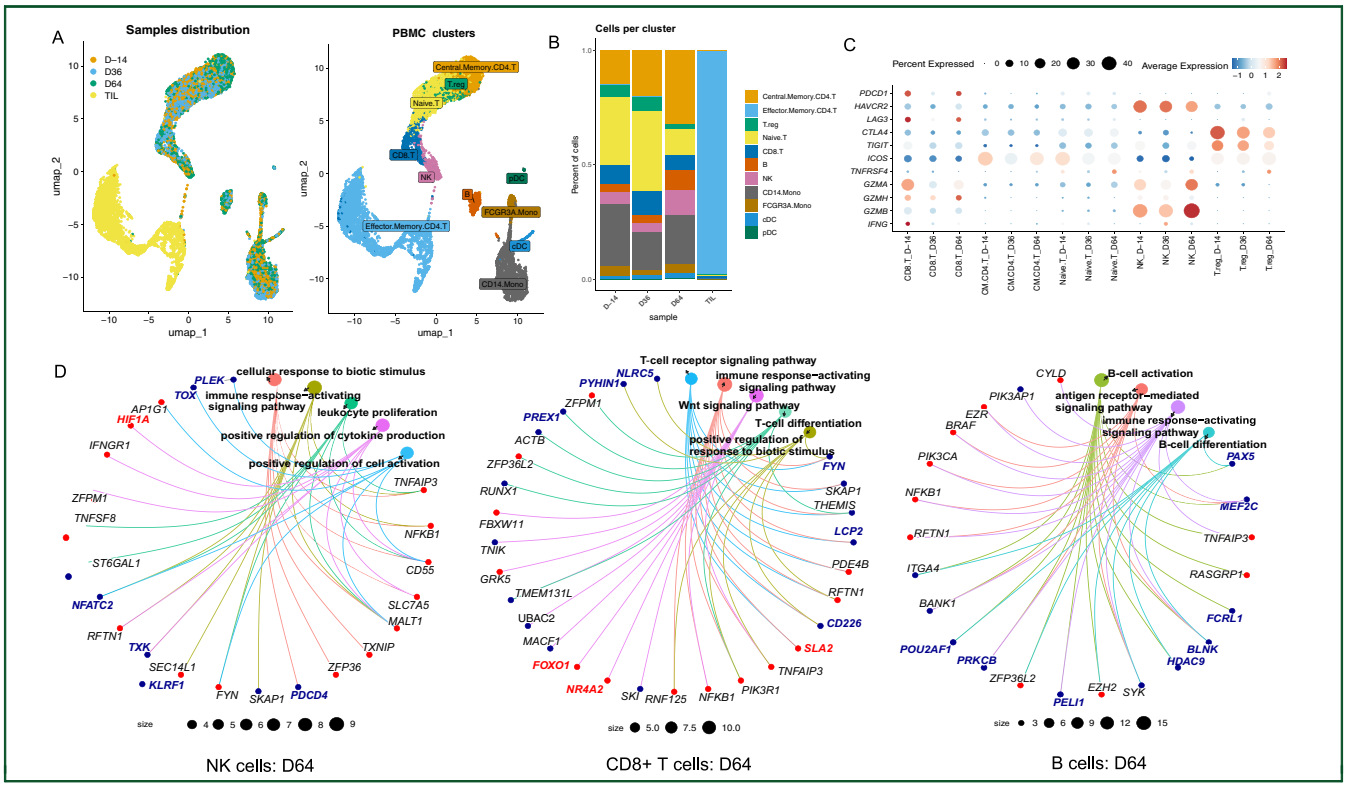

Figure 5. Analysis of immune cell populations in patients' peripheral blood mononuclear cells (PBMCs) collected on day −14 (D−14), day 36 (D36), and day 64 (D64). (A) Cell distribution within the samples. (B) Cell clustering carried out based on the expression of commonly used markers (Supplementary Figure S5, available at https://doi.org/10.1016/j.iotech.2024.100726). (C) Expression level of several cytotoxic and checkpoint markers per cluster in each sample. (D) Differentially expressed genes and significantly enriched gene ontology pathways in natural killer (NK), CD8+ T, and B cells on day 64.
CM, central memory.

observed increase in FOXP3-negative CD4+ T cells in the TME of the noninjected tumor following TIL infusion indicates that the infused TILs migrated to the tumor shortly after infusion. This is supported by a recent report showing that neoantigen-specific CD4+ T cells can be potent effector cells in TIL products.[16] The fact that the infused TILs were almost undetectable in peripheral blood shortly after infusion is, however, unusual. Previous studies show that neoantigen T cells in responding patients are detectable in peripheral blood for months or even years after TIL treatment.[17]

To this end, an increase in CD4+ cells in the TME of the noninjected tumor was observed even before TIL infusion, suggesting a contributory effect of OV therapy alone in promoting T-cell trafficking to the tumor site. This is confirmed by the fact that tumor regression in both injected and noninjected tumors was observed on day 36 before TIL administration. Indeed, an abscopal effect of TILT-123 injections has previously been reported.[18]

The fraction of CD8+ cells also increased in the TME of the noninjected tumor, particularly after TIL infusion. The fraction of CD8+ cells in the TIL infusion product was low (3.4%), but the absolute number of CD8+ cells was substantial (2.5×10^9 cells). Thus the observed increase in CD8+ cells within the TME, despite their low fraction in the TIL product, suggests a potential role in mediating the antitumor response.

In the virus-injected tumor, only day 64 biopsies were available. Nonetheless, the numbers of CD8+ and FOXP3-negative CD4+ cells in the TME were remarkedly high. This is in accordance with previous findings, reporting that TILT-123 is capable of inducing the trafficking of T cells into both injected and noninjected tumors.[18] This occurs through two mechanisms: the virus can spread systemically, and the immune response can be bodywide following the local presence of the virus.

In summary, based on the results from the IHC analyses, it is likely that an antitumor response was driven by CD8+ and CD4+ cells recruited by TILT-123 to the TME, potentiated by the large number of T cells present in the TIL product. In addition, the oncolytic effect of TILT-123 and the direct cell-killing effect of TNFα produced by the virus might have played a role.

We were not able to detect any *in vitro* tumor reactivity of the TILs against the tumor cell line or tumor digest. *Ex vivo* expansion of tumor cells might favor the growth of specific clones that are not dominant in the original tumor itself. Thus cancer cell lines are not necessarily good representatives of the tumor composition.[19] Besides, even though the clinical efficacy of TIL therapy, in general, is associated with detectable *in vitro* antitumor reactivity of TIL products, it is indeed not always the case on an individual patient level.[20]

The expression of PD-L1 in the TME increased from baseline to day 8 but decreased remarkedly from day 8 to day 64. The dynamics of PD-L1 expression is still a poorly understood area. In patients with non-small-cell lung cancer

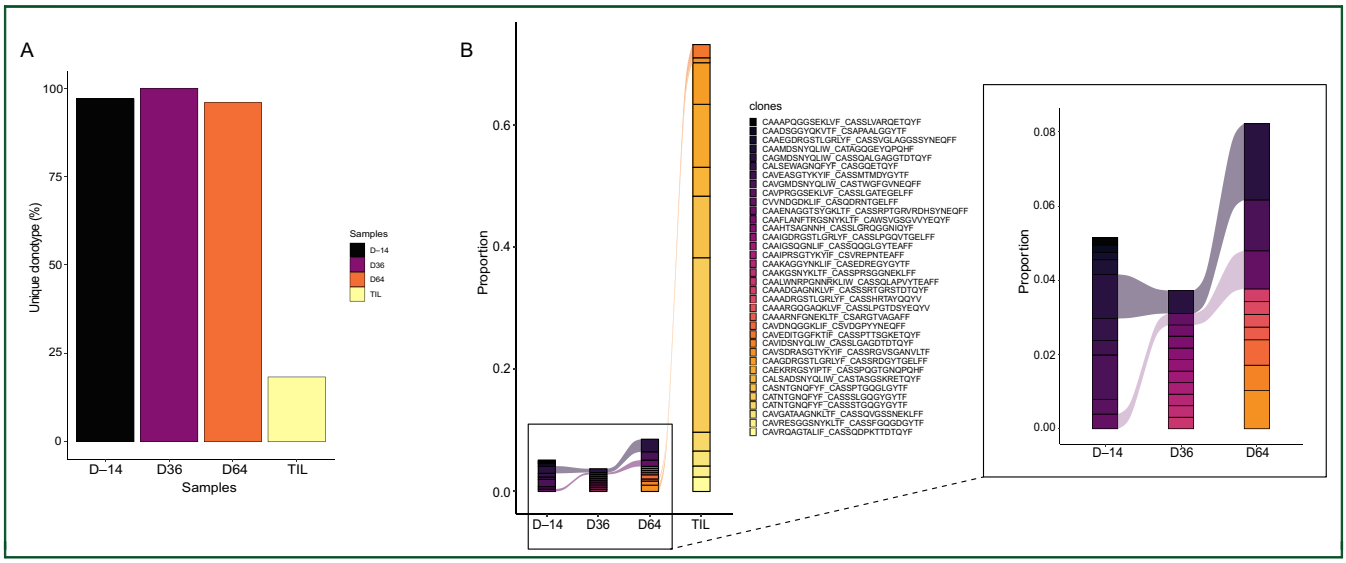

Figure 6. Clonotype diversity analysis of T-cell receptors (TCRs) in patients' peripheral blood mononuclear cells (PBMCs) and tumor-infiltrating lymphocyte (TIL) infusion product. (A) Percent of unique clonotypes in each sample. (B) Most abundant $\alpha\beta$TCR chains in TIL infusion product and PMBCs samples. D, day.

decreased PD-L1 expression during treatment with a PD-1 inhibitor was found to be associated with progressive disease.[14] However, PD-L1 expression might be highly heterogenous within the same tumor and the regulation of PD-L1 expression is affected by several factors, including the composition of the TME.

Analysis of T-cell receptor diversity showed a high clonality in the TIL product compared with peripheral blood. This is expected and reported previously.[21] None of the most expanded TCRs in the TIL product were previously described and their role remains unknown. Only one TCR clonotype was overlapping between PBMCs on day 64 and TILs, suggesting that most TILs did not stay in peripheral blood after infusion. The one clone persisting in peripheral blood after TIL infusion was not previously described.

Two different routes of administration (i.v. and i.t) were used for TILT-123. The optimal administration route for OVs is debated but, in general, the i.t. approach is the most widespread. However, i.v. dosing of OVs can also result in increased immune infiltration in solid tumors.[22] In the current case, the first TILT-123 injection was administered i.v. The purpose of this approach was to reach as many metastases as possible before the appearance of neutralizing antibodies. Indeed, we saw an increase in the titer of NABs 7 days after TILT-123 i.v. injection, suggesting a rapid development of humoral response toward the virus. The i.v. administration of TILT-123 was followed by the local i.t. administration that would, hopefully, boost the antitumor response while avoiding the NABs.

Single-cell analysis of PBMCs after TIL infusion showed that the number of CD4+ effector memory cells remained stable while the number of Tregs and naive T cells decreased remarkedly. The TIL infusion product comprised mostly CD4+ effector memory cells, indicating that the infused TILs migrated to the tumor site shortly after infusion. Thus the changes in the population of Tregs, naive T cells, NK cells, and B cells in peripheral blood were most likely induced by the OV therapy. Indeed, NK cells are known to be stimulated by OV therapy, and the transformation toward a more cytotoxic NK phenotype in the TME is expected upon viral therapy.[23]

In addition, analysis of cytotoxic markers on day 64 demonstrated a maturation of B cells and serum analysis showed increasing viral antibodies after i.v. administration. A well-described phenomenon associated with OV therapy is the induction of antiviral antibodies.[24] This humoral response against the virus supports the involvement and maturation of B cells detected in peripheral blood. Several reports are suggesting that the antiviral response contributes to the antitumor response through epitope spreading and local danger- and pathogen-associated signaling.[25,26]

Overall, from the translational data available it is not possible to rule out that the clinical response in this patient was driven exclusively by the OV therapy. However, based on the anatomic separation of the two lesions (injected and noninjected), local diffusion of OV would not be anticipated, thus abscopal efficacy of TILT-123 is possible. However, the contribution of the i.v. administered virus is difficult to clarify and the increased CD8+ and CD4+ T-cell infiltration of the TME of the noninjected tumor after TIL infusion indicates a contributory role of the TILs as well.

CONCLUSIONS

This case demonstrates that combined treatment with the OV TILT-123 and TIL therapy can result in a durable complete response in a patient with ICI-refractory metastatic mucosal melanoma located in the sinonasal cavity.

Immune profiling suggests that the response was driven by increased tumor infiltration of CD4+ and CD8+ cells—a process induced by TILT-123 and accelerated by the infusion of TILs. In addition, TILT-123-driven changes in the NK cell

phenotype in peripheral blood might have pushed the response further.

TCR sequencing revealed that the TIL product had high clonality and possessed mostly TCRs that were not previously described, underlining that TIL products are highly individualized and often multitargeted. Indications of clinical efficacy of the virus therapy alone were seen. However, the exact contribution of TILT-123 and TILs, respectively, to the response remains unclear.

Metastatic mucosal melanoma remains a diagnosis with limited treatment options and a poor prognosis. The current case demonstrates the potential of a combined immunotherapeutic approach in the search for more effective treatment modalities for these patients.

DISCLOSURE OF ARTIFICIAL INTELLIGENCE USE

During the preparation of this work, the authors used ChatGPT (OpenAI, San Francisco, CA) to increase the readability of some sections. After using this tool/service, the authors reviewed and edited the content as needed and take full responsibility for the content of the publication.

ACKNOWLEDGEMENTS

We thank Minna Oksanen, Susanna Grönberg-Vähä-Koskela, and Sini Raatikainen for expert assistance. This study was supported by Jane and Aatos Erkko Foundation, HUCH Research Funds (VTR), Cancer Foundation Finland, Sigrid Jusélius Foundation, Finnish Red Cross Blood Service, TILT Biotherapeutics Oy, University of Helsinki Doctoral Programme in Clinical Research, UNLEASHAD EU project. The authors extend their gratitude to Concept Life Sciences for conducting the multiplex immunofluorescence work, with special appreciation to Christopher Mills for his outstanding project management. Additionally, we thank OracleBio and IndicaLabs for their image analysis services.

DISCLOSURE

TJM has received honoraria for presentation from BMS and conference travel support from TILT Biotherapeutics Ltd. TK has received support for the present manuscript from the doctoral program in clinical cancer research, Medical Faculty, University of Helsinki in Finland, and from TILT Biotherapeutics Ltd. SP has received study material in support of the present manuscript from TILT Biotherapeutics Ltd. EE has received honoraria for lectures from Novartis, Merck, BMS, and Pierre Fabre; conference and travel support from Pierre Fabre and Merck. MD is receiving honoraria as an advisor of Achilles Therapeutics Limited; is a subinvestigator in a BMS clinical trial; is a member of the Danish Medicines Council (Medicinrådet) and Chairman of the Melanoma and Non-melanoma Skin Cancer Scientific Committee; and has proprietary data access in BMS and Genentech. RLE has received institutional drug funding from BMS for an investigator-initiated trial. CK is an employee and has stocks in TILT Biotherapeutics Ltd. JMS has received consulting payments and payment as an employee from TILT Biotherapeutics Ltd. in support for the present manuscript; support for conference attendance from TILT Biotherapeutics Ltd.; has a patent pending and stock options in TILT Biotherapeutics Ltd.; has received equipment (laptop) from TILT Biotherapeutics Ltd. JC is an employee at TILT Biotherapeutics Ltd.; has stock and stock options in TILT Biotherapeutics Ltd. LH is an employee and has stocks in TILT Biotherapeutics Ltd. DCAQ is an employee at TILT Biotherapeutics Ltd.; and has stock and stock options in TILT Biotherapeutics Ltd. RH is an employee at TILT Biotherapeutics Ltd.; and has stock options and RSUs in TILT Biotherapeutics Ltd. SS is an employee at TILT Biotherapeutics Ltd.; and has stock options in TILT Biotherapeutics Ltd. VCC has received payments for lectures/presentation/speaker bureaus/manuscript writing of educational events from TILT Biotherapeutics Ltd.; has patent planned from TILT Biotherapeutics Ltd.; has participated in data safety monitoring board or advisory board in TILT Biotherapeutics Ltd.; and has stocks in TILT Biotherapeutics Ltd. AH has issued and pending patents from TILT Biotherapeutics Ltd.; has received grants from Helsinki University Hospital Research funds; grants from Cancer Foundation Finland, Jane and Aatos Erkko Foundation, Red Cross Blood Service, and Sigrid Jusélius Foundation via the University of Helsinki; grant from the European Commission via TILT Biotherapeutics Oy; grant from TILT Biotherapeutics Oy for research support (reagents); salary contribution (for TK) in the doctoral program in clinical cancer research from the University of Helsinki; received research support via the University of Helsinki; is a shareholder in TILT Biotherapeutics Oy, Aeruginosa Oy, and Circio Holdings ASA. IMS has received grants for her institution from Evaxion Biotech, Adaptimmune, IO Biotech, Lytix Biopharma, TILT Biotherapeutics, Enara Bio, and Asgard Biotech; personal consulting fees from MSD, IO Biotech, Novartis, Pierre Fabre, and TILT Biotherapeutics; received payment for lectures from MSD, Novartis, sanofi-aventis, Pierre Fabre, BMS, Novo Nordisk, and Takeda; support for attending meetings and/or travel from MSD; has participated in data safety monitoring boards (for academic trials); has stocks in IO Biotech; and has received drugs for a clinical trial from BMS. All other authors have declared no conflicts of interest.

REFERENCES

1. Lawaetz M, Birch-Johansen F, Friis S, et al. Primary mucosal melanoma of the head and neck in Denmark, 1982—2012: demographic and clinical aspects. A retrospective DAHANCA study. *Acta Oncol*. 2016;55(8):1001-1008.
2. Li J, Kan H, Zhao L, Sun Z, Bai C. Immune checkpoint inhibitors in advanced or metastatic mucosal melanoma: a systematic review. *Ther Adv Med Oncol*. 2020;12:175883592092202.
3. Salari B, Foreman RK, Emerick KS, Lawrence DP, Duncan LM. Sinonasal mucosal melanoma: an update and review of the literature. *Am J Dermatopathol*. 2022;44(6):424-432.
4. Mikkelsen LH, Larsen AC, von Buchwald C, Drzewiecki KT, Prause JU, Heegaard S. Mucosal malignant melanoma — a clinical, oncological, pathological and genetic survey. *Apmis*. 2016;124(6):475-486.
5. Beaudoux O, Oudart JB, Riffaud L, et al. Mutational characteristics of primary mucosal melanoma: a systematic review. *Mol Diagnosis Ther*. 2022;26(2):189-202.

6. Rohaan MW, Borch TH, Kessels R, et al. Tumor-infiltrating lymphocyte therapy or ipilimumab in advanced melanoma. *N Engl J Med.* 2022;387(23):2113-2125.
7. Chandran SS, Somerville RPT, Yang JC, et al. Treatment of metastatic uveal melanoma with adoptive transfer of tumour-infiltrating lymphocytes: a single-centre, two-stage, single-arm, phase 2 study. *Lancet Oncol*. 2017;18(6):792-802.
8. Grigoleit G-U, Kluger H, Thomas S, et al. 1086MO Lifileucel tumor-infiltrating lymphocyte (TIL) cell therapy in patients (pts) with advanced mucosal melanoma after progression on immune checkpoint inhibitors (ICI): results from the phase II C-144-01 study. *Ann Oncol*. 2023;34(suppl 2):S654.
9. Olla D, Neumeister MW. Mucosal melanoma. *Clin Plast Surg*. 2021;48(4):707-711.
10. Shi T, Song X, Wang Y, Liu F, Wei J. Combining oncolytic viruses with cancer immunotherapy: establishing a new generation of cancer treatment. *Front Immunol*. 2020;11:683.
11. Chesney JA, Ribas A, Long GV, et al. Randomized, double-blind, placebo-controlled, global phase III trial of talimogene laherparepvec combined with pembrolizumab for advanced melanoma. *J Clin Oncol.* 2023;41(3):528-540.
12. Pakola SA, Peltola KJ, Clubb JHA, et al. Safety, Efficacy, and Biological Data of T-Cell—Enabling Oncolytic Adenovirus TILT-123 in Advanced Solid Cancers from the TUNIMO Monotherapy Phase I Trial. *Clin Cancer Res*. 2024. OF1-OF11. https://doi.org/10.1158/1078-0432.ccr-23-3874.
13. Donia M, Junker N, Ellebaek E, Andersen MH, Straten PT, Svane IM. Characterization and comparison of "standard" and "young" tumour-infiltrating lymphocytes for adoptive cell therapy at a Danish translational research institution. *Scand J Immunol*. 2012;75(2):157-167.
14. Zhao Y, Shi F, Zhou Q, et al. Prognostic significance of PD-L1 in advanced non-small cell lung carcinoma. *Med (United States)*. 2020;99(45):E23172.
15. Goncharov M, Bagaev D, Shcherbinin D, et al. VDJdb in the pandemic era: a compendium of T cell receptors specific for SARS-CoV-2. *Nat Methods*. 2022;19:1017-1019.
16. Hall MS, Teer JK, Yu X, et al. Neoantigen-specific CD4 + tumor-infiltrating lymphocytes are potent effectors identified within adoptive cell therapy products for metastatic melanoma patients. *J Immunother Cancer.* 2023;11(10):1-18.
17. Van Den Berg JH, Heemskerk B, Van Rooij N, et al. Tumor infiltrating lymphocytes (TIL) therapy in metastatic melanoma: boosting of neoantigen-specific T cell reactivity and long-term follow-up. *J Immunother Cancer.* 2020;8(2):1-11.
18. Havunen R, Santos JM, Sorsa S, et al. Abscopal effect in non-injected tumors achieved with cytokine-armed oncolytic adenovirus. *Mol Ther Oncolytics*. 2018;11:109-121.
19. Hynds RE, Vladimirou E, Janes SM. The secret lives of cancer cell lines. *DMM Dis Model Mech*. 2018;11(11):1-5.
20. Andersen R, Donia M, Ellebaek E, et al. Long-Lasting complete responses in patients with metastatic melanoma after adoptive cell therapy with tumor-infiltrating lymphocytes and an attenuated il2 regimen. *Clin Cancer Res.* 2016;22(15):3734-3745.
21. Lozano-Rabella M, Gros A. TCR repertoire changes during TIL expansion: clonal selection or drifting? *Clin Cancer Res*. 2020;26(16):4177-4179.
22. West EJ, Scott KJ, Tidswell E, et al. Intravenous oncolytic vaccinia virus therapy results in a differential immune response between cancer patients. *Cancers (Basel)*. 2022;14(9):1-15.
23. Warricker F, Khakoo SI, Blunt MD. The role of NK cells in oncolytic viral therapy: a focus on hepatocellular carcinoma. *J Transl Genet Genomics*. 2021;5(3):304-322.
24. Lemos de Matos A, Franco LS, McFadden G. Oncolytic viruses and the immune system: the dynamic duo. *Mol Ther Methods Clin Dev.* 2020;17:349-358.
25. Kanerva A, Nokisalmi P, Diaconu I, et al. Antiviral and antitumor T-cell immunity in patients treated with GM-CSF-coding oncolytic adenovirus. *Clin Cancer Res.* 2013;19(10):2734-2744.
26. Cervera-Carrascon V, Siurala M, Santos JM, et al. TNFa and IL-2 armed adenoviruses enable complete responses by anti-PD-1 checkpoint blockade. *Oncoimmunology.* 2018;7(5):1-11.